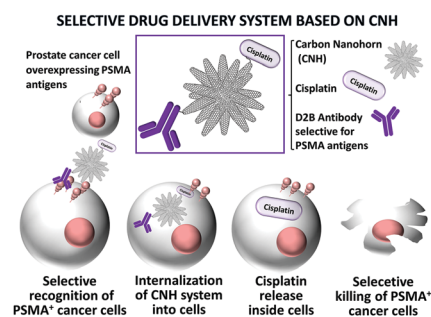


We have presented the Graphical Abstract text and image for your article below. This brief summary of your work will appear in the contents pages of the issue in which your article appears.



Targeted killing of prostate cancer cells using antibody–drug conjugated carbon nanohorns

María Isabel Lucio, Roberta Opri, Marcella Pinto, Alessia Scarsi, Jose L. G. Fierro, Moreno Meneghetti,* Giulio Fracasso,* Maurizio Prato, Ester Vázquez and María Antonia Herrero*

The ability of carbon nanohorns (CNHs) to cross biological barriers makes them potential carriers for delivery purposes.

Please check this proof carefully. **Our staff will not read it in detail after you have returned it.**

Proof corrections must be returned as a single set of corrections, approved by all co-authors. No further corrections can be made after you have submitted your proof corrections as we will publish your article online as soon as possible after they are received.

Please ensure that:

- The spelling and format of all author names and affiliations are checked carefully. Names will be indexed and cited as shown on the proof, so these must be correct.
- Any funding bodies have been acknowledged appropriately.
- All of the editor's queries are answered.
- Any necessary attachments, such as updated images or ESI files, are provided.

Translation errors between word-processor files and typesetting systems can occur so the whole proof needs to be read. Please pay particular attention to: tables; equations; numerical data; figures and graphics; and references.

Please send your corrections preferably as a copy of the proof PDF with electronic notes attached or alternatively as a list of corrections – do not change the text within the PDF file or send a revised manuscript. Corrections at this stage should be minor and not involve extensive changes.

Please return your **final** corrections, where possible within **48 hours** of receipt, by e-mail to: materialsB@rsc.org. If you require more time, please notify us by email.

Targeted killing of prostate cancer cells using
antibody–drug conjugated carbon nanohorns†

Cite this: DOI: 10.1039/c7tb02464a

María Isabel Lucío,^{abc} Roberta Opri,^d Marcella Pinto,^d Alessia Scarsi,^e
Jose L. G. Fierro,^f Moreno Meneghetti,^g *^e Giulio Fracasso,^g *^d
Maurizio Prato,^g *^{gh} Ester Vázquez,^g *^{ab} and María Antonia Herrero,^g *^{ab}

The ability of carbon nanohorns (CNHs) to cross biological barriers makes them potential carriers for delivery purposes. In this work, we report the design of a new selective antibody–drug nanosystem based on CNHs for the treatment of prostate cancer (PCa). In particular, cisplatin in a prodrug form and the monoclonal antibody (Ab) D2B, selective for PSMA⁺ cancer cells, have been attached to CNHs due to the current application of this antigen in PCa therapy. The hybrids Ab–CNHs, cisplatin–CNHs and functionalised–CNHs have also been synthesized to be used as control systems. The efficacy and specificity of the D2B–cisplatin–CNH conjugate to selectively target and kill PSMA⁺ prostate cancer cells have been demonstrated in comparison with other derivatives. The developed strategy to functionalise CNHs is fascinating because it can allow the fine tuning of both drug and Ab molecules attached to the nanostructure in order to modulate the activity of the nanosystem. Finally, the herein described methodology can be used for the incorporation of almost any drugs or Abs in the platforms in order to create new targeted drugs for the treatment of different diseases.

Received 13th September 2017,
Accepted 13th October 2017

DOI: 10.1039/c7tb02464a

rsc.li/materials-b

Introduction

Carbon nanohorns (CNHs) are in the shape of a single tube formed by a rolled graphene sheet with a closed horn-shaped tip. The tube has a diameter between 2 and 5 nm, a length of about 30–50 nm and normally self-assembles in spherical dahlia-like aggregates. These carbon nanostructures are emerging among others in nanomedicine due to their ideal homogeneous size (≈ 80 nm), which is useful for the cellular uptake,¹ and their synthesis in the absence of metal catalysts which could lead to undesired toxicity. In fact, CNHs have already

been used as carriers for drug,^{2,3} as well as genetic material,^{4,5} demonstrating that they are suitable platforms for delivery purposes. However, to date the main obstacle for the application of these nanomaterials is their lack of specificity.

Abs recognizing some tumour associated antigens (TAAs) are currently applied “naked”, conjugated to radiochemicals or to chemotherapeutic drugs in the clinics.⁶ They have also been used to improve the selectivity of carbon nanomaterials due to their easy conjugation to the nanostructures, the high affinity and stability,^{7–9} showing promising results in tumour diagnosis and therapy.¹⁰ Prostate cancer (PCa) is the most common cancer in man in industrialized countries and it can be often treated successfully when diagnosed in the early stages; local and regional stages show a 5 year relative survival rate nearly 100%.¹¹ Unfortunately patients where cancers have spread to distant lymph nodes, bones, or other organs show a drastic decrease of 5 year relative survival rate (*i.e.* survival rate of 28%), although some surgical, chemotherapeutic or radiotherapeutic treatments (*i.e.* alone or in combination) are performed. Therefore new therapeutical approaches are needed and, among these, the targeted approaches based on the recognition of cell associated tumour antigens are promising.¹²

Glutamate carboxypeptidase II (GCPII) is an enzyme expressed on the membrane of normal human prostate cells and at a very low level on duodenal epithelial (brush border) cells and proximal tubule cells in the kidneys.^{13–15} This enzyme, also called a prostate-specific membrane antigen (PSMA), is

^a Departamento de Química Orgánica, Inorgánica y Bioquímica, Facultad de Ciencias y Tecnologías Químicas, Universidad de Castilla-La Mancha, Campus Universitario, 13071 Ciudad Real, Spain. E-mail: MariaAntonia.Herrero@uclm.es

^b IRICA Universidad de Castilla-La Mancha, Campus Universitario, 13071 Ciudad Real, Spain

^c Department of Chemical and Pharmaceutical Sciences, University of Trieste, 34127 Trieste, Italy

^d Department of Medicine, University of Verona, Policlinico GB Rossi, Piazzale L.A. Scuro 10, 37134 Verona, Italy. E-mail: giulio.fracasso@univr.it

^e Department of Chemical Sciences, University of Padova, Via Marzolo, 1, II-35131, Padova, Italy. E-mail: moreno.meneghetti@unipd.it

^f Instituto de Catálisis y Petroleoquímica, CSIC, Cantoblanco, 28049, Madrid, Spain

^g CIC BiomaGUNE, Parque Tecnológico de San Sebastián, Paseo Miramón, 182, 20009 San Sebastián, Guipúzcoa, Spain

^h Basque Foundation for Science, Ikerbasque, Bilbao 48013, Spain

† Electronic supplementary information (ESI) available. See DOI: 10.1039/c7tb02464a

overexpressed in PCa tissues.¹⁶ PSMA is endowed with some fascinating characteristics: (i) an elevated level in metastatic and hormone refractory carcinomas; (ii) an influence on the survival and proliferation of prostate tumour cells^{17,18} and (iii) a peculiar expression on the neovasculature associated with other tumours.¹⁴ Therefore numerous efforts have been made in order to engineer specific antibodies against this antigen (Ag).^{19–21} Among these new Abs the clone called D2B, which recognizes extracellular domains of PSMA, shows very high affinity and a good “*in vitro*” and “*in vivo*” specificity as reported in many papers.^{22–24} Indeed, we have recently used the D2B antibody to build a sensor for the protein PSMA, as a prostate cancer biomarker, with very low limit of detection and quantification even in complex matrices.²⁵ The disadvantages of applying “naked” Abs in cancer passive immunotherapy are related to the down regulation of the target Ag in some tumour populations after the first set of treatments and/or the little efficacy of the immunological mechanisms activated after Ab–Ag recognition. These drawbacks have addressed the research to explore the potentiality of the Abs as a targeting moiety for drugs. Ab–drug conjugates represent an innovative therapeutic system that combines the leading properties of Abs with the cell killing activity of powerful cytotoxic drugs, reducing systemic toxicity and increasing the therapeutic benefit for patients.^{26–30} However, they would suffer from the same limitations of the “naked” antibodies.³¹ In addition, Ab–drug conjugates are not suitable for the incorporation of high loads of drug as this could imply a decrease of the Ab affinity to the target antigen. In this scenario CNHs could play an important role as cargo systems for the drug due to: (i) their easily multi-modifiable surface; (ii) their high cargo capacity; (iii) their accumulation in inflamed tissues also due to enhanced permeability and retention (EPR) effect. The design of selective drug nanocarriers has already been broached using non-covalent methodologies and showing targeted killing activity *in vitro* and *in vivo*.^{32,33}

Indeed nanotubes^{34–41} and nanohorns.^{2,42–45} have been applied to improve the uptake and selectivity of cisplatin, a well-known chemotherapeutic drug currently applied in the

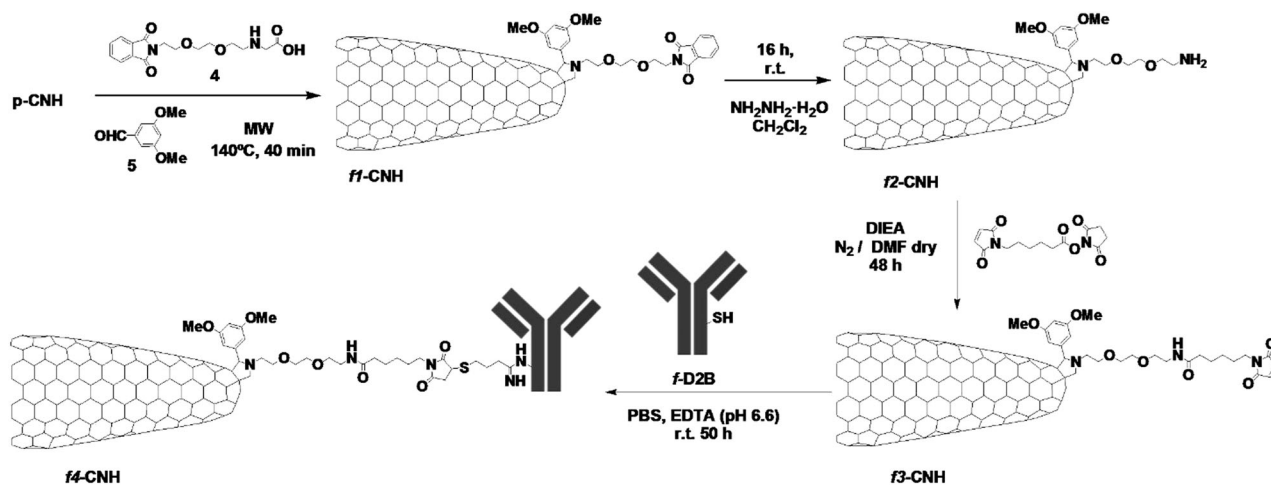
treatment of many solid tumours.⁴⁶ These delivery approaches highlight that covalent functionalization is an intriguing alternative to control the uptake and release of the drug. Furthermore, considering that the activity of platinum(II) drugs can be lost before arriving to cells,⁴⁷ the use of more inert platinum(IV) compounds as prodrugs are springing up to avoid deactivation.⁴⁸ In fact, carbon nanotubes have been previously studied as carriers for Pt(IV) prodrugs, which release Pt(II) inside the cells by the reduction caused by low-pH of the tumour microenvironment and intracellular organelles as endosomes.⁴⁹

In this way, we are taking into account the feasible orthogonal multi-functionalization of CNHs previously optimized in our lab⁵⁰ and their excellent properties to act as delivery systems in order to obtain selective drugs. Concretely, the objective of this work was the design of a new CNH based platform which carries an antineoplastic agent (cisplatin) together with a targeting moiety, the anti-PSMA D2B Ab, for the specific intoxication of PCa cells. Other derivatives were synthesized together with our hybrid Ab–CNH–drug in order to have a comparative analysis of their behaviour in cells (*i.e.* functionalised CNHs without Ab and drug and CNHs functionalised only with drug or with Ab). All the complexes were fully characterized using various techniques, such as UV-Vis-NIR spectroscopy, Raman spectrometry, transmission electron microscopy (TEM) and thermogravimetric analysis (TGA), and finally, they were assayed to investigate the selectivity and activity towards cancer cells.

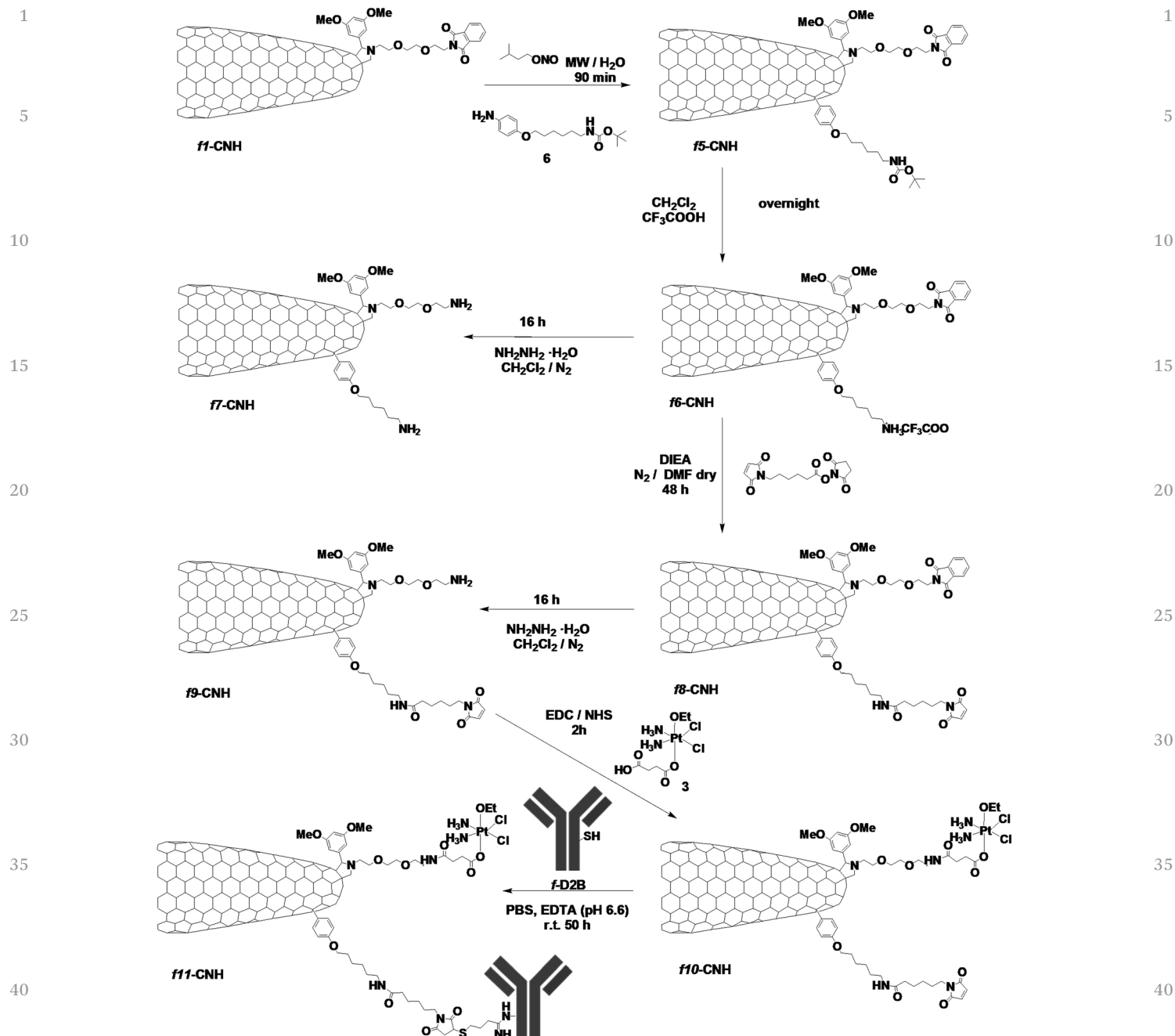
Results and discussion

Synthesis of the α -amino acid, aniline, the prodrug and modification of the D2B antibody

The α -amino acid 4 and aniline 6 (Schemes 1 and 2) were used for the double functionalization of CNHs *via* 1,3-dipolar cycloaddition and radical addition. They were chosen in order to have two different protected groups that can be selectively deprotected and long chains that could afford solubility. Their synthesis was carried out according to the literature.^{50–53}



Scheme 1 Synthesis of functionalised carbon nanohorns f4-CNH.



Scheme 2 Synthesis of functionalised carbon nanohorns f7-CNH, f10-CNH and f11-CNH.

The Pt(IV) prodrug 3 was synthesized following the previously described procedure (Fig. S1, ESI†).⁵⁴ Cisplatin was firstly oxidized in ethanolic hydrogen peroxide under N_2 affording intermediate 2 in 98% yield. In the next reaction, the hydroxide of the complex reacted with succinic anhydride under N_2 producing the cisplatin derivative 3 in 35% yield, capable of being attached to an amine-functionalised CNH through the carboxyl group. This prodrug 3 is able to release the toxic molecule cisplatin upon intracellular reduction caused by the low pH environment.⁵⁴

The chosen methodology to attach the Abs to the CNHs is the addition of thiol groups on the previously inserted

maleimide chains. Therefore, modification of D2B Ab was performed applying 2-iminothiolane (2-IT, Traut's reagent) in order to increase the number of accessible thiol groups.⁵⁵ The amount of thiols was determined by Ellman's assay⁵⁶ showing an average of one thiol group per antibody.

Synthesis and characterisation of carbon nanohorn derivatives

Ab-CNT derivatives have demonstrated to bind specific target Ags on cancer cells in a selective way. The choice of creating a covalent bond can provide a more chemically stable conjugate and prevent the premature release of the Abs due to their

1 **Table 1** Functionalization data based on TGA results and the qualitative Kaiser test

Sample	TGA, N ₂ , weight loss at 600 °C	μmol F.G. per g CNHs (TGA)	μmol amino group per g CNHs Kaiser test
f2-CNH	15%	484	121
f3-CNH	18%	336	≈0
f4-CNH	34%	1.06 ^a	n/a
f5-CNH	23%	308 ^b	≈0
f6-CNH	20%	319 ^b	100
f7-CNH	17%	257 ^c	139
f8-CNH	23%	194 ^d	≈0
f9-CNH	22%	110 ^c	118

^a Number of antibodies. ^b Chains of functional groups introduced by the radical addition of anilines. ^c Chains of functional groups introduced by 1,3-dipolar cycloaddition. ^d Chains of introduced maleimide groups.

exchange with other proteins present in serum, onto the nanotube surface.^{25,57} Therefore, we used this approximation to build similar hybrids with CNHs.

As a first approach, the synthesis of the Ab-functionalised CNHs was addressed (Scheme 1). Firstly, we carried out a 1,3-dipolar cycloaddition on the pristine carbon nanohorns (p-CNH) using the phthalimide-protected amino acid 4 and aldehyde 5 under microwave irradiation.⁵⁰ Then, a basic medium (hydrazine in dichloromethane) was applied to deprotect the necessary amine groups for the next step. The thermogravimetric analysis of the f2-CNH sample showed a weight loss of 15% at 600 °C under N₂ (Fig. S2, ESI;† Table 1,) corresponding to 484 μmol of functional group per gram of carbon nanohorns and it was consistent with the positive Kaiser test (121 μmol of amino groups per g CNH), which determines the free amine groups in organic compounds.⁵⁸

The low value of the Kaiser tests in comparison with the TGA data is attributed to the low solubility of the carbon nanostructures which prevents the titration of all the amino compounds by UV-Vis-NIR spectroscopy. The posterior reaction of f2-CNH with 6-maleimidoheptanoic acid *N*-hydroxysuccinimide (NHS) ester yielded the f3-CNH intermediate (18% weight loss, N₂, 600 °C, Fig. S2, ESI,† Table 1), corresponding to 336 μmol of the functional group per gram of CNHs and the negative Kaiser test. This hybrid incorporates a maleimide group for the next binding to sulfhydryl groups of the Ab.

In the last stage, the thiolated Ab (f-D2B) was attached to the maleimido groups by reaction in PBS-EDTA (4 μM) at pH = 6.6, for 60 h. The reaction was carried out at this pH to avoid hydrolysis of the maleimido group⁵⁷ and regeneration of 2-IT.⁵⁹ The success of the addition was demonstrated by the absence of free thiol groups in the crude of reaction by Ellman's test. After cleaning with PBS-EDTA (4 μM), f4-CNH was analysed by thermogravimetric analysis, observing a weight loss of 34% at 600 °C under N₂ (Fig. S2, ESI;† Table 1), corresponding to 1.06 μmol of Ab per gram of CNHs.

Once the synthesis of Ab-CNH f4-CNH was achieved, the synthesis of the hybrid Ab-CNH-drug f11-CNH was carried out. The derivatives without Ab and drug (f7-CNH) and the one with drug but without Ab (f10-CNH) were synthesized *via* the same

synthetic route (control samples). The preparation of all hybrids is summarized in Scheme 2.

In a first step, starting from the derivative functionalised by 1,3-dipolar cycloaddition of f1-CNH, a new chain with an orthogonal protective group 6 was introduced in CNHs following the same procedure previously described by our group.⁵⁰ The yielded hybrid f5-CNH possesses two different protected focal points which allow the incorporation of different molecules. Based on TGA analysis (Fig. S4, ESI;†) we introduced 308 μmol of the Boc-protected functional group per gram of CNHs in the arene radical addition on the nanohorns previously functionalised with a phthalimide-protected functional group. This implies the introduction of 1 Boc-protected functional group every approximately 190 carbon atoms, a value that agrees with the previously reported ones.⁵⁰ These data were calculated from the difference between the total weight loss and the weight loss after 1,3-dipolar cycloaddition in TGA.

Afterwards, selective deprotection of Boc-protected amines in acid media was carried out yielding the f6-CNH derivative. The Kaiser test yielded 100 μmol of free amines per gram of CNHs and TGA yielded 319 μmol of the functional group per gram of CNHs (Fig. S3, ESI;† Table 1). The data from the TGA were calculated according to the removed organic material, the difference between the weight loss of the protected derivative and the deprotected one. The posterior deprotection of these nanohorns in a basic medium turned out to be f7-CNH with 139 μmol of total free amines per gram of CNHs according to the Kaiser test. The TGA yielded the release of 257 amines (Fig. S3, ESI;† Table 1). The f7-CNH derivative has enhanced solubility in comparison with pristine CNHs. The decrease in weight loss observed for the deprotected derivatives f6-CNH and f7-CNH (blue and red lines in Fig. S4, ESI;†) agrees with the removal of the organic material in every deprotection step.

Continuing with the preparation of the CNH derivatives, a 6-maleimidoheptanoic acid NHS ester was added to f6-CNH to obtain the focal point for the posterior union of the Ab in f8-CNH. Then, phthalimide was selectively eliminated from f8-CNH by reaction in a basic medium, yielding the necessary intermediate f9-CNH to attach prodrug 3. The TGA and Kaiser test results of f8-CNH and f9-CNH are summarized in Table 1. In this case, TGA and Kaiser test data agree probably as a consequence of the increased solubility of these materials.

Prodrug 3 was finally attached to f9-CNH yielding the f10-CNH derivative. This reaction was carried out in the absence of light in order to avoid undesirable reactions of the prodrug. Derivatives f9-CNH and f10-CNH were analysed by TGA under air (Fig. S4, ESI;†). Using this method the amount of metal in the sample can be detected after complete oxidation. The introduction of 44 μmol of drug per gram of CNHs in f10-CNH was calculated from TGA (Table 2).

Further proof of the incorporation of the platinum compound in the nanohorns was achieved by the analysis of the derivative f10-CNH using X-ray photoelectron spectroscopy (XPS). This is a semi-quantitative technique that provides information about the elemental composition of the sample as well as about the existent types of bonds.⁶⁰ The Pt 4f

1 Table 2 Amounts of Ab or cisplatin per gram of CNHs

Sample	μmol antibody per g CNHs	μmol cisplatin per g CNHs
f4-CNH	1.06	n/a ^a
f7-CNH	n/a ^a	n/a ^a
f10-CNH	n/a ^a	44
f11-CNH	1.47	44

^a n/a indicates there is no drug or Ab in the hybrid.

spectrum of f10-CNH satisfactorily fitted with two doublets in which the most intense peak of everyone (Pt 4f_{7/2}) appeared at 73.3 and 74.7 eV, demonstrating the presence of platinum in the sample. An energy of 73.5 eV has been previously assigned to the Pt 4f_{7/2} component of Pt 4f in pure PtCl₂ in which Pt is in the Pt(II) form and energies between 74.6 and 75 eV have been assigned to PtO₂ and H₂PtCl₆ compounds in which Pt is in its Pt(IV) form.⁶⁰ On the other hand, the presence of peaks associated with Pt(II) compounds in the spectra of Pt(IV) compounds was also expected as it has been previously reported that the exposure of Pt(IV) complexes to X-ray radiation using MgK α irradiation (the one uses in our experiment) causes a reduction of Pt(IV) into Pt(II).⁶¹

In the last stage, the thiolated Ab previously synthesized was attached to the maleimido groups by reaction in PBS-EDTA (4 μM) for 60 h yielding the f11-CNH derivative. The pH of the reaction medium was 6.6 as in the previous synthesis of f4-CNH. In the same way, the success of the addition was demonstrated by the absence of free thiol groups in the crude of reaction by Ellman's test. After cleaning by filtration, f11-CNH was analysed by thermogravimetric analysis in N₂, observing a weight loss of 44% at 600 °C under N₂, corresponding to 1.47 μmol of Ab per gram of CNHs (Fig. S5, ESI[†]; Table 2).

Furthermore, the f11-CNH derivative was also analysed by XPS. The Pt 4f_{7/2} spectrum of this sample was also fitted with two doublets at 73.3 and 74.7 eV according to the presence of the platinum prodrug. Interestingly, a peak at 164.3 eV in the spectrum indicated the presence of S 2p nuclei in the sample, which are due to the presence of the Ab (Fig. S6, ESI[†]).

All the synthesized derivatives were analysed by transmission electron microscopy (TEM) to complete the characterization. No changes were observed in the spherical morphology of CNHs after functionalization. In addition, improvement in dispersion with increasing degree of functionalization was perceived (Fig. 1).

As an overview, the presence of cisplatin and Ab in biologically significant compounds is summarized in Table 2.

Interaction with cells

As previously highlighted, the main objective of this work was to selectively target drugs towards cancer cells. So to investigate whether our hybrids were able to achieve this goal, the biological properties of the complexes f4-CNH, f7-CNH, f10-CNH and f11-CNH were analysed. In this way, different techniques were used in order to check the binding specificity, uptake and cytotoxicity of these different nanosystems. Moreover the presence of D2B Ab on the surface of the different hybrids was analysed to confirm their correct functionalization.

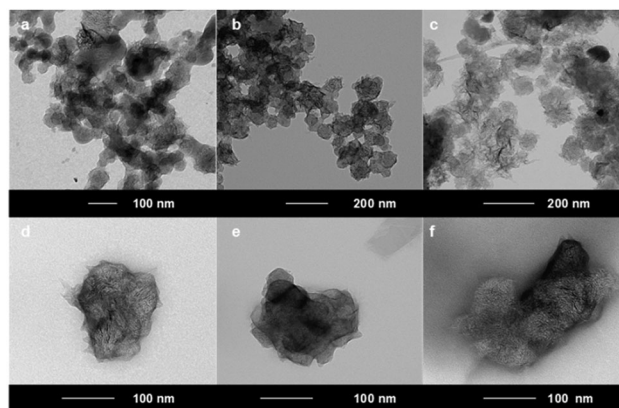


Fig. 1 TEM images of p-CNH (a), f4-CNH (b), f7-CNH (c), f10-CNH (d) and f11-CNH in H₂O solution (e) and PBS solution (f).

Flow cytometry was used to investigate the presence of D2B antibody on the CNH surface.

Flow cytometry was applied to analyse the interaction between cells and nanostructures (*i.e.* binding and uptake) and also to check if the Abs are linked to the CNH surface. Therefore, to demonstrate that the Abs are bound to the nanosystems, we applied a goat-anti-mouse Ab FITC labelled (Gam-FITC) which is able to recognize the murine D2B Ab. As negative control we analysed f7-CNH not conjugated with D2B Ab. The FITC fluorescence signal observed on f11-CNH, Fig. 2b (mean fluorescence intensity, MFI value = 33.994), demonstrated the presence of Abs on the CNH surface. The very low autofluorescence and scattering signals of f11-CNH alone are depicted in Fig. 2a (MFI value = 65). Moreover, a modest signal was observed with the negative control f7-CNH stained with the Gam-FITC reagent (Fig. 2c, MFI value = 476), probably due to limited non-specific absorption of the stain Ab-FITC on the nanosystem surface. Positive signals, similar to those observed with f11-CNH, were obtained by analysing the f4-CNH hybrid (*i.e.* drug unloaded and Ab conjugated), demonstrating the presence of Abs on the CNH surface (data not shown).

Raman spectroscopy. The strong intensity of the Raman signals from carbon nanostructures is a useful tool to identify them in cells⁷ and tissues.^{5,6} Moreover, the Raman technique has the advantages of being a non-destructive technique and it does not need external contrast-enhancing agents. Taking this into account, the ability of CNH hybrids to interact with different cancerous cells was analysed by Raman spectroscopy.

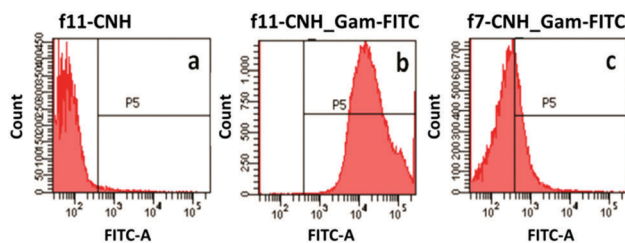


Fig. 2 Flow cytometry analysis of: (a) f11-CNH alone, (b) f11-CNH stained with the Gam-FITC reagent, (c) f7-CNH (no Ab conjugated, negative control) stained with the Gam-FITC reagent.

CNHs can be identified by Raman spectroscopy due to the presence of two characteristic bands at around 1600 (G-band) and 1320 (D-band) cm^{-1} , related, respectively, to the sp^2 π -conjugated carbons and to the sp^3 non-conjugated carbons considered to be defects of the CNH structure; furthermore their strong absorption/scattering makes it possible to identify them also with optical images in which dark spots can be observed where they accumulate. Raman spectra were registered at a single-cell level after 3 h of CNH incubation with cells. Firstly, the spectra of PC-3-PSMA cells alone were recorded and they clearly do not show the typical CNH Raman signature (Fig. 3b, cell 2 and 3); the spectra of the glass slide were also recorded (*i.e.* background signal, Fig. 3b, point 1). In Fig. 3c and d, active targeting of PC-3-PSMA cells using f4-CNH (concentration of $62.5 \mu\text{g mL}^{-1}$) was observed. The images, observed using an optical microscope ($20\times$ magnification) of the μ -Raman instrument, allow us to see dark spots in many cells (Fig. 3c). The Raman spectrum collected on these cells clearly identifies the characteristic spectrum of CNHs (Fig. 3d). Conversely, the cell image of Fig. 3e shows that in A431 cells dark spots are almost absent. Correspondingly, a low intensity CNH spectrum can be observed only for the few cells for which some spots are observed (Fig. 3f). This shows that specific interactions are almost absent in A431 (PSMA⁻) cells treated with f4-CNH at the same concentration ($62.5 \mu\text{g mL}^{-1}$).

Once the ability of f4-CNH (*i.e.* D2B-CNHs) to selectively bind PSMA⁺ cancer cells was demonstrated, the next step was to

analyse the binding capability of f11-CNH (*i.e.* CNHs conjugated to Ab and drug). High f11-CNH accumulation was observed in PC-3-PSMA cells under an optical microscope (black spots in Fig. S7, ESI[†]). Moreover, Raman spectroscopy spectra collected at a single-cell level from randomly selected cells showed the characteristic Raman signature of CNHs (Fig. S7, ESI[†]) demonstrating the presence of nanostructures and, therefore, the uptake into these Ag⁺ cells.

Binding analysis of the different hybrids on PSMA^{+/-} cells by flow cytometry. In a subsequent series of experiments, the binding and specificity of f11-CNH (D2B-CNHs) were analysed by flow cytometry on both PC-3-PSMA and PC-3 wild type (WT, PSMA⁻) cells at different CNH concentrations (Table 3). In these assays we used the Gam-FITC reagent to show the binding (*i.e.* at 4 °C) of CNHs on PSMA^{+/-} cells. With this protocol we detected the binding of the derivatives to the cells staining D2B Ab linked to the CNH surface.

As expected, when PSMA⁺ cells were incubated with increasing concentration of the f11-CNH derivative they showed a gain of the Gam-FITC (*i.e.* secondary antibody) staining with respect to the staining of the cells with Gam-FITC alone (*i.e.* without CNH incubation, control signal); conversely, any increment of the signal with respect to the control was observed when increasing concentrations of f11-CNH were incubated with PSMA⁻ cells and stained with GAM-FITC (*i.e.* PC-3 WT cells, Table 3). Moreover, a CNH sample was also washed by centrifugation to change the buffer to be sure that the positive signals were detected when the f11-CNH derivative was incubated with PSMA⁺ cells were not due to the presence of traces of free Ab in the batch. When a pre-centrifuged f11-CNH dispersion at $250 \mu\text{g mL}^{-1}$ was incubated with PC-3-PSMA cells and stained with Gam-FITC the normalized MFI value was quite superimposable to the value obtained using the same f11-CNH dispersion not washed by centrifugation. (*i.e.* 17.2 versus 17.7 for the washed and unwashed f11-CNH, respectively). Thus the fluorescent signal detected by flow cytometry is absolutely due to the binding of f11-CNH on the cell surface.

Afterward, a saturation experiment was carried out at +4 °C to better investigate the binding capability of f11-CNH on PC-3-PSMA cells (Fig. 4). PSMA Ag saturation was reached at an f11-CNH concentration of about $200 \mu\text{g mL}^{-1}$ (*i.e.* D2B-CNH); this saturation curve allowed us to confirm the specific binding of f11-CNH to the PSMA⁺ cells.

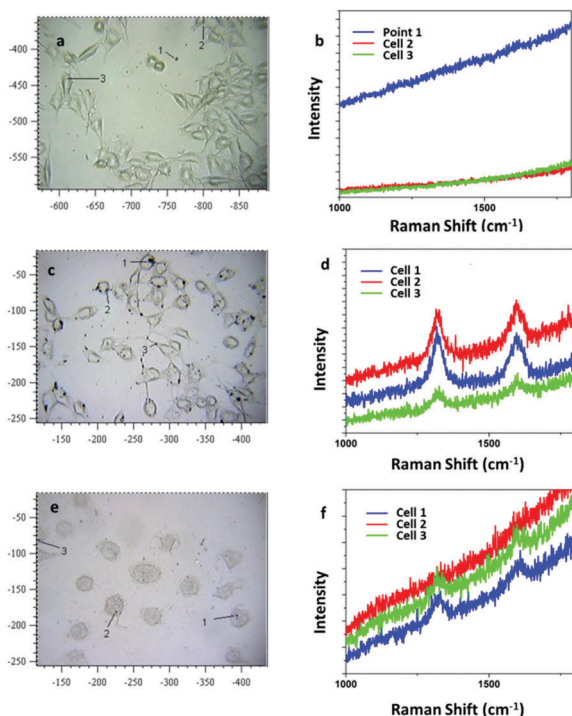


Fig. 3 Bright-field microscopy images and Raman spectra collected at 633 nm of PC-3-PSMA cells alone (a and b), PC-3-PSMA cells incubated with f4-CNH at $62.5 \mu\text{g mL}^{-1}$ (c and d) and A431 cells, PSMA⁻, incubated with f4-CNH at $62.5 \mu\text{g mL}^{-1}$ (e and f). When present, the two bands can be identified as the D and G bands at 1320 and 1600 cm^{-1} , respectively.

Table 3 Binding at 4 °C for 1 h of f11-CNH serial dilution on PSMA^{+/-} cells. MFI values obtained by flow cytometry were normalized to obtain the fluorescent signal gain with respect to the signal of the cells incubated with the secondary antibody FITC-labelled alone (*i.e.* MFI sample/MFI Gam-FITC; see the Experimental section for more details). Mean \pm SD data of three separate experiments

CNHs, $\mu\text{g mL}^{-1}$	PC-3-PSMA cells	PC-3 WT (PSMA ⁻) cells
	f11-CNH	f11-CNH
62.5	8.8 ± 1.0	0.9 ± 0.1
125	14.0 ± 1.0	0.8 ± 0.5
250	17.7 ± 0.7	0.7 ± 0.5

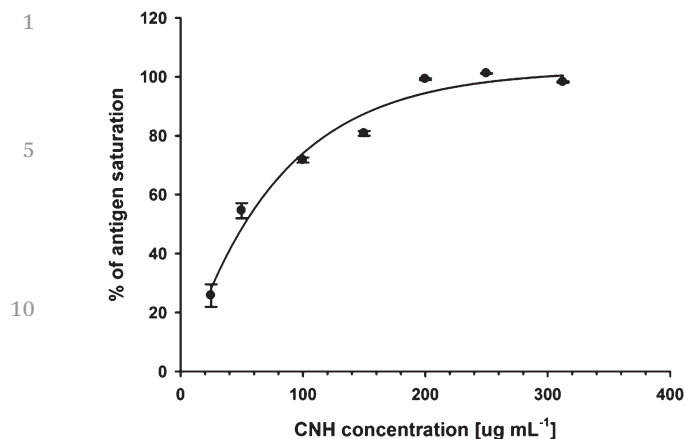


Fig. 4 Saturation binding curve of f11-CNH at 4 °C on PC-3-PSMA cells.

Additionally, a competition binding assay was performed to strongly confirm the binding specificity of f11-CNH hybrids on PSMA⁺ cells. We analysed the binding signals of a fixed concentration of biotinylated D2B Ab to PC-3-PSMA cells in the presence of f11-CNH serial dilution. The decrease of the fluorescence signal associated with the cells stained with streptavidin-RPE-D2B-biotin complex *versus* the CNH concentrations is shown in Fig. S8, ESI[†]; it is observed that when the concentration of the f11-CNH hybrid is increased, a reduction of D2B-biotin staining occurs. So a competition between the f11-CNH hybrid and free biotinylated Ab, D2B-biotin is demonstrated, for PSMA sites located on the cell surface and consequently the PSMA specificity of our targeted f11-CNH hybrid.

Uptake analysis of the different hybrids into PSMA^{+/-} cells by flow cytometry. The binding to Ag⁺ cells is not enough to increase the targeted/drug-loaded CNH killing specificity and their cytotoxicity; therefore their entrance into the cells is mandatory. In fact, overcoming the cellular membrane is actually one of the main tasks of the CNHs in the complexes. In order to show that the uptake of f11-CNH into cells was achieved and not only the binding to the cell surface, new flow cytometric analyses were carried out on permeabilized and intact cells. Therefore we compared fluorescence signals of permeabilized and not permeabilized cells after incubation with two different f11-CNH concentrations and staining with the Gam-FITC reagent. As summarized in Table 4, the normalized MFI value on permeabilized cells is remarkably higher (*i.e.* signal from bound and internalised CNHs) than the signal on

Table 4 Evaluation of binding and uptake of f11-CNH on PC-3-PSMA cells after incubation for 1 h 30 min at 37 °C. MFI values obtained by flow cytometry were normalized to obtain the fluorescent signal gain with respect to the signal of the cells incubated with the secondary antibody FITC-labelled alone (*i.e.* MFI sample/MFI Gam-FITC; see the Experimental section for more details). Mean \pm SD data of three separate experiments

f11-CNH, µg mL ⁻¹	Binding	Uptake
125	11.2 \pm 1.6	20.9 \pm 0.1
250	17.5 \pm 1.6	41.8 \pm 1.0

non-permeabilized ones (*i.e.* signal from only bound CNHs) at each analysed f11-CNH concentration. Therefore, a significant number of CNHs did not only bind to the cell surface but were also internalised into the cells.

In order to confirm this observation, the same experiment was performed on a second PSMA⁺ cell line, LNCaP cells, and the obtained data agree with those measured on PC-3-PSMA cells (Table S1, ESI[†]). Moreover the experiment was replicated on PC-3 WT cells, PSMA⁻ cells, where no binding and no internalisation were observed (Table S2, ESI[†]).

***In vitro* evaluation of the cytotoxic effects.** The main goal of the f11-CNH derivative is to selectively kill PSMA⁺ cancer cells. In order to assess this property, the *in vitro* cytotoxicity of different CNH derivatives (f10-CNH and f11-CNH) was evaluated on PSMA⁺ cells.

As summarized in Table 5, when PC-3-PSMA cells were treated with 2.2 µM in cisplatin of the CNH derivatives, we observed a quite similar toxicity (see a percentage of cell viability around 0.1–0.5%); conversely when we increased the stealth properties of the CNH derivatives by a preadsorption step with BSA (*i.e.* bovine serum albumin) the percentage of cell viability of f10-CNH increased to 66.72 \pm 1.78% and the same data remained below 20% for f11-CNH. Under the same conditions (plus and minus BSA preadsorption), when cells were treated with 2.2 µM of cisplatin alone, the percentage of cell viability was about 95%. The dose-response curves of PC-3-PSMA cells treated for 24 h at 37 °C with serial dilution of cisplatin, f10-CNH and f11-CNH, with and without the BSA preadsorption step, can be observed in Fig. S9 and S10, ESI[†].

The non-specific toxicity caused by f10-CNH is clearly due to an incomplete masking of the CNH surface; in fact when the stealth properties were increased by protein absorption, the specificity of f11-CNH was improved with respect to the f10-CNH derivative. Additionally, when PC-3 WT cells, PSMA⁻, were treated with f11-CNH (*i.e.* cisplatin concentration 1.1 µM) without BSA pre-coating, the percentage of viable cells was 77.60 \pm 6.66%, whereas the cell viability of PSMA⁺ cells dropped to 28.31 \pm 3.55% when incubated with the same derivative concentration.

According to these results, our target hybrid f11-CNH is able to more selectively kill PSMA⁺ cancer cells in contrast to the cisplatin-functionalised carbon nanohorns without antibody (*i.e.* f10-CNH). Moreover it is also important to highlight that the killing efficacy of the same dose of cisplatin was dramatically increased when carried to the tumour cells by the Ab-CNHS.

Table 5 Cytotoxicity data of f10-CNH, f11-CNH and cisplatin on PC-3-PSMA⁺ cells. Data summarize the killing efficacy obtained using 2.2 µM concentration in cisplatin with or without the addition of BSA to increase the CNH stealth properties. Mean \pm SD data of three separate experiments

Sample	PC-3-PSMA (PSMA ⁺)	
	Minus BSA	Plus BSA
f10-CNH	0.46 \pm 0.31%	66.72 \pm 1.78%
f11-CNH	0.1 \pm 0.22%	19.31 \pm 0.80%
Cisplatin	96.33 \pm 3.38	95.90 \pm 0.91

1 The cytotoxicity data, obtained when BSA pre-incubation was per-
formed, suggest that increased CNH stealth properties by coating
with PEG chains (*i.e.* pegylation),⁶² with disordered polypeptide
chains comprising the small residues Pro, Ala and Ser (*i.e.*
5 PASylation),⁶³ or with biomimetic leukocyte membranes,⁶⁴ could
lead to a nanosystem with improved selectivity.

Experimental section

Synthesis and characterization of carbon nanohorn derivatives

10 **Techniques.** Microwave irradiation was carried out on a
CEM Discover reactor, with an infrared pyrometer, a pressure
control system, and stirring and air-cooling options. UV-vis-NIR
15 experiments were carried out on a Varian Cary 5000 spectro-
photometer. Thermogravimetric analyses (TGA) were per-
formed using a TGA Q50 (TA Instruments) at 10 °C min⁻¹
under N₂. For transmission electron microscopy (TEM) several
drops of CNH solutions in MeOH (2.5 × 10⁻² mg mL⁻¹) were
20 placed on a copper grid (3.00 mm, 200 mesh, coated with
carbon film). After being dried under high vacuum overnight,
the sample was investigated by TEM using a Philips EM 208
with an accelerating voltage of 100 kV. Photoelectron spectra
(XPS) were obtained using a VG Escalab 200R spectrometer
25 equipped with a hemispherical electron analyser with a pass
energy of 50 eV and a Mg K α ($h\nu = 1254.6$ eV) X-ray source,
powered at 120 W. Binding energies were calibrated relative to
the C 1s peak at 284.8 eV. High-resolution spectra envelopes
were obtained by curve fitting synthetic peak components using
30 the software "XPS peak." Symmetric Gaussian-Lorentzian
curves were used to approximate the line shapes of the fitting
components. Atomic ratios were computed from experimental
intensity ratios and normalized by atomic sensitivity factors.
1H-NMR and 13C-NMR spectra were recorded in solvent on a
35 Varian Inova 400 spectrometer operating at 399.78 MHz for 1H
and 100.53 for 13C. The values of the chemical shift (δ) are
quoted in parts per million (ppm) and the coupling constants
(J) in Hertz (Hz).

40 **Materials.** Solvents were purchased from SDS and Fluka.
Chemicals were purchased from Sigma-Aldrich and used as
received without further purification. CNHs were purchased
from Carbonium s.r.l. (Padova, Italy) and used without purifi-
cation. Amino acid 4 and aniline derivative 6 were synthesized
45 following the literature procedure.⁵⁰⁻⁵³

50 **Synthesis of *c,c,t*-[Pt(NH₃)₂Cl₂(OH)(OEt)], 2.** In absence of
light, *cis*-[Pt(NH₃)Cl₂] (0.20 g, 0.67 mmol) was suspended in
absolute EtOH (250 mL) and heated to 70 °C. A solution of H₂O₂
(0.5 mL, 50%) was added to this suspension with vigorous
55 stirring. After 5 h at elevated temperature the solid dissolved to
afford a bright yellow solution. After cooling at room tempera-
ture, the solution volume was reduced to near dryness on a
rotary evaporator and Et₂O (50 mL) was added to precipitate the
product as a light yellow solid. The solid was collected and
washed with ice cold EtOH and Et₂O. The yield was 98% (0.236
g, 0.65 mmol). 1H-NMR (500 MHz, [D₆]-DMF, 25 °C): $\delta = 10.44$ (s,

1H, OH); 6.018 (s, br, 6H, NH₃); 3.58 (q, 2H, CH₂); 1.10 ppm (q,
3H, CH₃). m.p. 172–175 °C.

5 **Synthesis of *c,c,t*-[Pt(NH₃)₂Cl₂(OEt)(O₂CCH₂CH₂CO₂H)], 3.**
Compound 2 (5 × 10⁻² g, 0.14 mmol) was dissolved in 2 mL
of dry DMF. Succinic anhydride (2.1 × 10⁻² g, 0.21 mmol) in dry
DMF (1 mL) was added to this solution and the solution was
stirred for 4 h at 75 °C under N₂. The resulting solution was
dried under vacuum to obtain dark yellow oil, which was
dissolved in a small amount of acetone. Addition of Et₂O
10 precipitated a solid that was collected and dried under vacuum
to leave the product as a pale yellow powder in 35% yield (2.3 ×
10⁻² g, 0.05 mmol). 1H-NMR (500 MHz, [D₆]-DMF, 25 °C): $\delta =$
12.36 (m, 1H, CO₂H); 6.14 (m, 6H, NH₃); 3.52 (s, 2H, CH₂); 2.95
15 (s, 2H, CH₂); 2.78 (s, 2H, CH₂); 1.01 ppm (t, 3H, CH₃). m.p.
(decomposition), 120–124 °C.

20 **Modification of the antibody (f-D2B).** 1.17 mg of EDTA were
added to a D2B solution (1 mL, 1.5 mg mL⁻¹) in PBS to afford 4
mM and NaHCO₃ saturated (0.1 mL). A freshly prepared
solution of 2-iminothiolane-HCl in water (10 μ L, 2 mg mL⁻¹)
25 was added. The mixture was shaken for 2 h at 30 °C, and then it
was incubated over night at 4 °C. Finally, the excess of 2-IT was
removed by dialysis (MWCO = 500–1000 Da) against PBS/EDTA
4 mM. The number of free sulfhydryl groups introduced in f-
D2B was assessed by Ellman's assay to be approximately 1
30 per Ab.

35 **Synthesis of f1-CN_H.** Pristine CNHs (25 mg) were suspended
in CH₂Cl₂ (5 mL) with aldehyde 5 (110 mg, 0.66 mmol) and
amino acid 4 (211 mg, 0.66 mmol) in a microwave quartz vessel;
after sonication for 5 min, the solvent was evaporated under a
N₂ stream, the vessel was closed and introduced into mono-
mode microwave where the mixture was irradiated for 45 min at
different powers and temperatures.⁵⁰ After this period of time,
the crude was re-suspended in 75 mL of CH₂Cl₂ and sonicated
35 for 5 min. The solution was filtered on a Millipore membrane
(PTFE, 0.2 μ m) and the collected black solid was washed with
cycles of sonication and filtration using three different mix-
tures of solvents: (i) 100 mL of MeOH/HCl (37%) in proportion
3: 1, (ii) 75 mL of MeOH and (iii) 75 mL of CH₂Cl₂ (sonicated
40 and filtered) and finally dried under high vacuum affording 24
mg of f1-CN_H.

45 **Synthesis of f2-CN_H.** f1-CN_H (30 mg) were suspended in
CH₂Cl₂ (30 mL) with hydrazine (9 mL, 0.06 mol) and the
mixture was stirred for 16 h at room temperature under N₂.
The crude was filtered on a Millipore membrane (PTFE, 0.2 μ m)
and washed by cycles of sonication and filtration with CH₂Cl₂
50 (75 mL) and MeOH (100 mL), and finally dried under high
vacuum affording 28 mg of f2-CN_H.

55 **Synthesis of f3-CN_H.** f2-CN_H (13 mg, 6.5 μ mol of amine
groups) were suspended in dry DMF (5 mL) and neutralized
with dry DIEA (57 μ L, 325 μ mol) under N₂. A solution of 6-
maleimidohexanoic acid *N*-hydroxysuccinimide ester (40 mg,
130 μ mol) in DMF (2 mL) was added. The reaction was
55 sonicated for 20 min and then stirred at r.t. under N₂ for

1 48 h. The obtained f3-CNH was extensively washed by filtration
(on a Millipore membrane (PTFE, 0.2 μm) with DMF, MeOH
and Et₂O, and then dried under high vacuum). Yield: 13 mg.

5 *Synthesis of f4-CNH.* The maleimido-derivated f3-CNH (10
mg) was dispersed in PBS/EDTA (20 mL, 4 mM) and the f-D2B
solution (3.6 mL, 2 μM) was added and the mixture was shaken
for 60 h at r.t. The obtained f4-CNH was washed by filtration on
a Millipore membrane (PTFE, 0.2 μm) with PBS. The resulting
10 Ab-conjugate f4-CNH was stored at 4 °C as dispersions of 0.5
mg mL⁻¹ in PBS (pH 7.4). The solubility was around 0.4 mg
mL⁻¹ in PBS/EDTA (4 mM).

15 *Synthesis of f5-CNH.* f1-CNH (40 mg) were sonicated in
deionized water together with Boc-protected aniline 6 (1.53 g,
6.92 mmol) for 10 min in a microwave glass vessel. Finally,
isoamyl nitrite (0.44 mL, 3.34 mmol) was added, and a con-
denser was placed. The mixture was irradiated at 80 °C with
20 monomode microwave working at 100 W for 30 min, and after
the addition of a new aliquot of isoamyl nitrite (0.44 mL,
3.34 mmol), at 30 W for 60 min. After cooling at room
temperature, the crude was filtered on a Millipore membrane
(GTFP, 0.2 μm). The collected black solid was washed using
25 cycles of sonication and filtration with MeOH until the filtrate
was clear and finally dried under high vacuum affording 36 mg
of double functionalised intermediate f5-CNHs.

30 *Synthesis of f6-CNH.* The double protected intermediated (f5-
CNH, 90 mg) was sonicated in CH₂Cl₂ (100 mL) for 5 min.
Then, trifluoroacetic acid (100 mL) was added. The mixture was
stirred for 48 h at room temperature. The crude was filtered on
the Millipore membrane (PTFE, 0.2 μm) and washed by cycles
of sonication and filtration with CH₂Cl₂ (75 mL) and Et₂O (50
mL), and finally dried under high vacuum affording 80 mg of
f6-CNH.

35 *Synthesis of f7-CNH.* f6-CNH (12 mg) were suspended in
CH₂Cl₂ (12 mL) with hydrazine (3.6 mL, 0.024 mol) and the
mixture was stirred for 16 h at room temperature. The crude
was filtered on a Millipore membrane (PTFE, 0.2 μm) and
40 washed by cycles of sonication and filtration with CH₂Cl₂ (75
mL) and MeOH (100 mL) and Et₂O (50 mL), and finally dried
under high vacuum affording 10.5 mg of f7-CNH.

45 *Synthesis of f8-CNH.* f6-CNH (60 mg, 13.75 μmol of amine
groups) were suspended in dry DMF (5 mL) and neutralized
with dry DIEA (200 μL , 1140.35 μmol) under N₂. A solution of 6-
maleimido-hexanoic acid NHS ester (85 mg, 276.25 μmol) in
DMF (4 mL) was added. The reaction was sonicated for 10 min
and then stirred at room temperature under N₂ for 48 h. The
50 obtained f8-CNH was extensively washed by filtration on a
Millipore membrane (PTFE, 0.2 μm) with DMF, MeOH and
Et₂O, and then dried under high vacuum affording 56 mg of f8-
CNH.

55 *Synthesis of f9-CNH.* f8-CNH (52 mg) were suspended in
CH₂Cl₂ (52 mL) with hydrazine (15.6 mL, 0.1 mol) and the
mixture was stirred for 16 h at room temperature. The crude

was filtered on a Millipore membrane (PTFE, 0.2 μm) and
washed by cycles of sonication and filtration with CH₂Cl₂ (75
mL) and MeOH (100 mL) and Et₂O (50 mL), and finally dried
under high vacuum affording 45 mg of f9-CNH.

5 *Synthesis of f10-CNH.* In the absence of light, an aqueous
solution of *N*-hydroxysuccinimide (NHS) (20 mL, 1.0 mM) was
added to an equal volume of an aqueous 1.0 mM solution of 1-
ethyl-3-[3-dimethylaminopropyl]carbodiimide hydrochloride (EDC)
and the resulting solution was allowed to stand at room tempera-
10 ture for 10 min. *c,c,t*-[Pt(NH₃)₂Cl₂(OEt)(O₂CCH₂CH₂CO₂H)] 3 (7 mg)
in MQ water was added to this solution. After 10 min, f9-CNH (42
mg) were added. The solution was sonicated for 3 min, heated to
50 °C for 2 h and then agitated overnight at room temperature. The
crude was filtered on a Millipore membrane (GTFP, 0.2 μm) and
15 washed with MQ water. 40 mg of f10-CNH were obtained.

20 *Synthesis of f11-CNH.* The maleimido-derivated f10-CNH (18
mg) was dispersed in PBS/EDTA (20 mL, 4 mM) and an f-D2B
solution (17 mL, 6.7 μM) was added. The mixture was shaken
for 60 h at room temperature until no Ab was detected in the
supernatant by UV-Vis-NIR spectroscopy. Finally, the resulting
f11-CNH was washed by filtration on a Millipore membrane
(PTFE, 0.2 μm) with PBS. The resulting Ab-conjugate f11-CNH
was stored at 4 °C as dispersions of 0.25 mg mL⁻¹ in PBS/EDTA
25 (pH 7.8).

Interaction with cells

30 **Raman spectroscopy.** Different cell lines, PC-3-PSMA PCa
cells (*i.e.* transfected to express the PSMA antigen) and A431
35 cells (PSMA⁻) were incubated with 62.5 $\mu\text{g mL}^{-1}$ of f4-CNH at
37 °C for 3 h and then, after washing and fixating with 2%
paraformaldehyde, Raman spectra were recorded at a single-
cell level using a 20 \times objective and a controlled XY stage using
a Renishaw inVia confocal μ -Raman instrument equipped with
35 a He-Ne laser. A power lower than 1 mW at 633 nm was used for
excitation.

40 **Cell lines and anti-PSMA antibody.** PC-3 WT (human pros-
tate tumour cells, PSMA⁻), LNCaP (human prostate tumour
cells, PSMA⁺) and A431 (human epidermoid carcinoma cells,
45 PSMA⁻) were obtained from American Type Culture Collection
(ATCC, Manassas, VA, Rockville, USA). PC-3-PSMA cells (*i.e.* also
called PC-3-PIP) stably transfected to express human PSMA
were kindly provided by Dr Warren Heston (Department of
Cancer Biology, Cleveland Clinic Main Campus).²³ PC-3, PC-3-
50 PSMA and LNCaP cells were cultured in RPMI 1640 Medium
supplemented with 2 mM L-glutamine and 0.01 M HEPES and
maintained at 37 °C in a humidified atmosphere containing 5%
CO₂ and 90% of humidity. A431 cells were cultured in DMEM
medium with the same reagents and also with 1 mM Na pyruvate.
55 Moreover all the media were supplemented with 10% heat-
inactivated foetal bovine serum (FBS) (Invitrogen, New York,
NY, USA) and antibiotics (0.1 mg mL⁻¹ streptomycin and 100
units mL⁻¹ penicillin G (Sigma-Aldrich, St Louis, MO, USA)).

The anti-PSMA mouse antibody D2B was purified from the
hybridoma supernatant by affinity chromatography on Protein

1 G Sepharose 4 Fast Flow (GE Helthcare Europe GmbH, Milano, Italy).

2 **Detection of the D2B-Ab on the CNH surface by flow**
3 **cytometry.** We applied flow cytometry to confirm the presence
4 of the Ab on the CNH surface; briefly f11-CNH, f4-CNH and f7-
5 CNH were incubated with a goat anti-mouse (Gam) antibody,
6 FITC-labelled (BD Biosciences, Milan, Italy), for 1 h at 4 °C in
7 PBS plus BSA 0.2%. Then CNHs were washed with cold PBS and
8 the bound fluorescence was analysed using a BD FACSCanto II
9 apparatus (BD Biosciences).

Analysis of CNH interaction with cells by flow cytometry

10 **Binding.** In these assays to show the binding (*i.e.* at 4 °C for 1
11 h) of the CNHs to PSMA^{+/−} cells we used a goat anti-mouse
12 (Gam) antibody FITC-labelled (*i.e.* Gam-FITC reagent); negative
13 cells were applied to confirm also the target specificity. Due to
14 the variability of the non-specific binding of the secondary
15 antibody FITC-labelled to the cell lines under analysis, we
16 decided to normalize the inter-experimental data measuring
17 the fluorescent signal gain of our samples with respect to the
18 signal of the cells incubated with the secondary antibody FITC-
19 labelled alone (*i.e.* MFI sample/MFI Gam-FITC). Using the Gam-
20 FITC for the flow cytometry analysis we recognised the deriva-
21 tives bound to the cells staining the D2B Ab linked to the CNH
22 surface. To be sure that the positive signals observed in the flow
23 cytometry analysis were not due to the presence of free D2B
24 antibody in the f11-CNH batch, we also analysed a sample that
25 was centrifuged before the analysis to change the buffer and
26 eliminate free D2B antibody, if present. Briefly, 200 000 cells
27 were incubated at 4 °C for 1 h with three different concentra-
28 tions of f11-CNH (*i.e.* 62.5, 125 and 250 µg mL^{−1}) and then,
29 after two washing steps, stained with the Gam-FITC reagent.
30 Finally, CNHs were washed with cold PBS and the fluorescence
31 associated with the cells was analysed using the flow cytometer.
32 The same protocol was applied to create the saturation binding
33 curve of f11-CNH to PC-3-PSMA cells where dilutions ranging
34 from 25 to 500 µg mL^{−1} were used.

35 **Competition-binding.** In the competition-binding experi-
36 ment the same number of cells was co-incubated with different
37 derivative concentrations, ranging from 0 µg mL^{−1} to 375 µg
38 mL^{−1}, and 1 µg of D2B-biotin Ab for 1 h at 4 °C, then samples
39 were washed twice with cold PBS buffer and incubated with
40 streptavidin-RPE (streptavidin labelled with *R*-phycoerythrin)
41 for 30 min at 4 °C. After a washing step the samples were
42 analysed using the flow cytometer.

43 **Uptake vs. binding.** Cells were plated on a 24 well per plate.
44 Then, cells were incubated the day after with two concentra-
45 tions of f11-CNHs for 1 h 30 min at 37 °C. They were washed
46 with PBS buffer and detached with PBS-EDTA. For each experi-
47 mental point a portion of the total cells was permeabilized with
48 70% MeOH for 1 h in ice and then incubated with Gam-FITC
49 for FACS analysis. The residual cells, no permeabilized, were
50 also incubated with Gam-FITC; at the end of the incubation,
51 cells were washed with cold PBS and analysed using a flow
52 cytometer. The binding signal is given by CNHs bound to the
53 PSMA antigen on the no permeabilized cells (*i.e.* surface signal

alone) conversely. The uptake data were obtained from the
permeabilized cells where we have the addition of both signals
due to the CNHs internalised and the CNHs bound to the cell
surface.

54 **Viability assay.** For the viability assays cells were seeded, one
55 day before the assay, at an appropriate cell density in 90 µL of
complete medium in 96 well culture microplates; the day after,
the cells were incubated in triplicate with 10 µL of serial
dilution of f11-CNHs, f10-CNHs or Cisplatin alone at 37 °C
for 22 h. Then, the cells were washed and incubated for 2 h in
the medium supplemented with the XTT reagent (Sigma-
Aldrich), according to the supplier instructions; finally cell
viability was measured at 450 nm using a microplate reader.
The percent of cell viability was estimated analysing the values
obtained from treated cells with respect to mock treated ones.

Conclusions

20 A new series of hybrid materials composed of carbon nano-
21 horns as delivery vehicles (Ab-CNH, drug-CNH, Ab-drug-CNH
22 and double functionalised-CNH) have been synthesized and
23 fully characterized. In particular, cisplatin in a prodrug form
24 and a specific D2B antibody for PSMA⁺ prostate cancer cells
25 have been attached. Different biological experiments have
26 demonstrated the selective binding and uptake of the conju-
27 gates with antibody (Ab-CNH and Ab-drug-CNH) on PSMA⁺
28 prostate cancer cells. Finally, the selectivity of the derivative
29 Ab-drug-CNH on PSMA⁺ prostate cancer cells has made possi-
30 ble their selective killing *versus* PSMA[−] prostate cancer cells.
31 This property is enhanced when the nanosystems are shielded
32 with BSA. In conclusion, we have demonstrated the better
33 ability of f11-CNH to selectively kill PSMA⁺ cancer cells in
34 comparison with the other synthesized CNH hybrids. Further-
35 more, this new system offers great potentiality due to the
36 possibility of modifying the type and degree of functionaliza-
37 tion. This allows the variation of the quantity of drug or anti-
38 body attached to the nanostructure in order to play with the
39 killing efficacy. Similarly, the method is useful to attach differ-
40 ent drugs or antibodies opening the way to the treatment of
41 other diseases.

Conflicts of interest

42 There are no conflicts to declare.

Acknowledgements

43 G. F. gratefully acknowledges Fondazione Cariverona, Verona
44 Nanomedicine Initiative and Italian Minister of Health RF-
45 2010-2305526 for supporting this work. M. M. thanks the
46 University of Padova (P-DiSC #04BIRD2016-UNIPD). This work
47 was also supported by the Spanish Ministry of Economy and
48 Competitiveness MINECO (projects CTQ2014-53600-R and
49 CTQ2016-76721-R), by the EU Graphene-based disruptive tech-
50 nologies, Flagship project (no. 696656). M. P., as the recipient

of the AXA Chair, is grateful to the AXA Research Fund for financial support. M. P. was also supported by Diputación Foral de Gipuzkoa program Red (101/16).

Notes and references

- 1 S. Lacotte, A. García, M. Décossas, W. T. Al-Jamal, S. Li, K. Kostarelos, S. Muller, M. Prato, H. Dumortier and A. Bianco, *Adv. Mater.*, 2008, **20**, 2421–2426.
- 2 K. Ajima, M. Yudasaka, T. Murakami, A. Maigne, K. Shiba and S. Iijima, *Mol. Pharmaceutics*, 2005, **2**, 475–480.
- 3 T. Murakami, K. Ajima, J. Miyawaki, M. Yudasaka, S. Iijima and K. Shiba, *Mol. Pharmaceutics*, 2004, **1**, 399–405.
- 4 F. C. Pérez-Martínez, B. Carrión, M. I. Lucío, N. Rubio, M. A. Herrero, E. Vázquez and V. Ceña, *Biomaterials*, 2012, **33**, 8152–8159.
- 5 J. Guerra, M. A. Herrero, B. Carrión, F. C. Pérez-Martínez, M. I. Lucío, N. Rubio, M. Meneghetti, M. Prato, V. Ceña and E. Vázquez, *Carbon*, 2012, **50**, 2832–2844.
- 6 G. J. Weiner, *Nat. Rev. Cancer*, 2015, **15**, 361–370.
- 7 Y. Xiao, X. Gao, O. Taratula, S. Treado, A. Urbas, R. D. Holbrook, R. E. Cavicchi, C. T. Avedisian, S. Mitra, R. Savla, P. D. Wagner, S. Srivastava and H. He, *BMC Cancer*, 2009, **9**, 1–11.
- 8 J. Kim, E. I. Galanzha, E. V. Shashkov, H. Moon and V. P. Zharov, *Nat. Nanotechnol.*, 2013, **4**, 688–694.
- 9 R. Marega, F. De Leo, F. Pineux, J. Sgrignani, A. Magistrato, A. D. Naik, Y. Garcia, L. Flamant, C. Michiels and D. Bonifazi, *Adv. Funct. Mater.*, 2013, **23**, 3173–3184.
- 10 F. Riedel, I. Zaiss, D. Herzog, K. Götte, R. Naim and K. Hörmann, *Anticancer Res.*, 2005, **25**, 2761–2766.
- 11 www.cancer.org/cancer/prostatecancer/detailedguide/prostate-cancer-survival-rates.
- 12 M. Kuroki and N. Shirasu, *Anticancer Res.*, 2014, **34**, 4481–4488.
- 13 G. P. Murphy, T. G. Geene, W. T. Tino, A. L. Boyton and E. H. Holmes, *J. Urol.*, 1998, **160**, 2396–2401.
- 14 S. S. Chang, D. S. O. Keefe, D. J. Bacich, V. E. Reuter, W. D. W. Heston and P. B. Gaudin, *Clin. Cancer Res.*, 1999, **5**, 2674–2681.
- 15 H. Liu, P. Moy, S. Kim, Y. Xia, A. Rajasekaran, V. Navarro, B. Knudsen and N. H. Bander, *Cancer Res.*, 1997, **57**, 3629–3634.
- 16 R. G. Lapidus, C. W. Tiffany, J. T. Isaacs and B. S. Slusher, *Prostate*, 2000, **45**, 350–354.
- 17 M. Colombatti, S. Grasso, A. Porzia, G. Fracasso, M. T. Scupoli, S. Cingarlini, O. Poffe, H. Y. Naim, M. Heine, G. Tridente, F. Mainiero and D. Ramarli, *PLoS One*, 2009, **4**, e4608.
- 18 M. E. Perico, S. Grasso, M. Brunelli, G. Martignoni, E. Munari, E. Moiso, G. Fracasso, T. Cestari, H. Y. Naim, V. Bronte, M. Colombatti and D. Ramarli, *Oncotarget*, 2016, **7**, 74189–74202.
- 19 X. Wang, L. Yin, P. Rao, R. Stein, K. M. Harsch, Z. Lee and W. D. W. Heston, *J. Cell. Biochem.*, 2007, **102**, 571–579.
- 20 S. S. Taneja, *Rev. Urol.*, 2004, **6**, 19–28.
- 21 M. Meneghetti, A. Scarsi, L. Litt, G. Marcolongo, V. Amendola, M. Gobbo, M. Di Chio, A. Boscaini, G. Fracasso and M. Colombatti, *Small*, 2012, **8**, 3733–3738.
- 22 J. Tykvart, V. Navrátil, F. Sedlák, E. Corey, M. Colombatti, G. Fracasso, F. Koukolík, C. Bařinka, P. Sacha and J. Konvalinka, *Prostate*, 2014, **74**, 1674–1690.
- 23 B. Frigerio, G. Fracasso, E. Luison, S. Cingarlini, M. Mortarino, A. Coliva, E. Seregni, E. Bombardieri, G. Zuccolotto, A. Rosato, M. Colombatti, S. Canevari and M. Figini, *Eur. J. Cancer*, 2013, **49**, 2223–2232.
- 24 S. Lütje, C. M. van Rij, G. M. Franssen, G. Fracasso, W. Helfrich, A. Eek, W. J. Oyen, M. Colombatti and O. C. Boerman, *Contrast Media Mol. Imaging*, 2014, **10**, 28–36.
- 25 A. Juzgado, A. Soldà, A. Ostric, A. Criado, G. Valenti, S. Rapino, G. Conti, G. Fracasso, F. Paolucci and M. Prato, *J. Mater. Chem. B*, 2017, **5**, 6681–6687.
- 26 J. R. Adair, P. W. Howard, J. A. Hartley, D. G. Williams and K. A. Chester, *Expert Opin. Biol. Ther.*, 2012, **12**, 1191–1206.
- 27 S. Chen and Y. Cao, *JSM Cell*, 2014, **2**, 1006.
- 28 P. D. Senter, *Curr. Opin. Chem. Biol.*, 2009, **13**, 235–244.
- 29 P. J. Carter and P. D. Senter, *Cancer J.*, 2008, **14**, 154–169.
- 30 A. G. Polson, J. Calemene-Fenaux, P. Chan, W. Chang, E. Christensen, S. Clark, F. J. de Sauvage, D. Eaton, K. Elkins, J. M. Elliott, G. Frantz, R. N. Fujii, A. Gray, K. Harden, G. S. Ingle, N. M. Kljavin, H. Koeppen, C. Nelson, S. Prabhu, H. Raab, S. Ross, D. S. Slaga, J.-P. Stephan, S. J. Scales, S. D. Spencer, R. Vandlen, B. Wranik, S.-F. Yu, B. Zheng and A. Ebens, *Cancer Res.*, 2009, **69**, 2358–2364.
- 31 P. Chames, M. Van Regenmortel, E. Weiss and D. Baty, *Br. J. Pharmacol.*, 2009, **157**, 220–233.
- 32 X. Ma, C. Shu, J. Guo, L. Pang, L. Su, D. Fu and W. Zhong, *J. Nanopart. Res.*, 2014, **16**, 2497.
- 33 N. Li, Q. Zhao, C. Shu, X. Ma, R. Li, H. Shen and W. Zhong, *Int. J. Pharm.*, 2014, **478**, 644–654.
- 34 C. Tripisciano and E. Borowiak-Palen, *Phys. Status Solidi*, 2008, **245**, 1979–1982.
- 35 C. Tripisciano, K. Kraemer, A. Taylor and E. Borowiak-Palen, *Chem. Phys. Lett.*, 2009, **478**, 200–205.
- 36 C. Tripisciano, S. Costa, R. J. Kalenczuk and E. Borowiak-Palen, *Eur. Phys. J. B*, 2010, **75**, 141–146.
- 37 L. Sui, T. Yang, P. Gao, A. Meng, P. Wang, Z. Wu and J. Wang, *Int. J. Pharm.*, 2014, **471**, 157–165.
- 38 J. Li, S. Q. Yap, S. L. Yoong, T. R. Nayak, G. W. Chandra, W. H. Ang, T. Panczyk, S. Ramaprabhu, S. K. Vashist, F.-S. Sheu, A. Tan and G. Pastorin, *Carbon*, 2012, **50**, 1625–1634.
- 39 J. Li, A. Pant, C. F. Chin, W. H. Ang, C. Ménard-Moyon, T. R. Nayak, D. Gibson, S. Ramaprabhu, T. Panczyk, A. Bianco and G. Pastorin, *Nanomedicine*, 2014, **10**, 1465–1475.
- 40 S. L. Yoong, B. S. Wong, Q. L. Zhou, C. F. Chin, J. Li, T. Venkatesan, H. K. Ho, V. Yu, W. H. Ang and G. Pastorin, *Biomaterials*, 2014, **35**, 748–759.
- 41 W. Wu, R. Li, X. Bian, Z. Zhu, D. Ding, X. Li, Z. Jia, X. Jiang and Y. Hu, *ACS Nano*, 2009, **3**, 2740–2750.

- 1 42 K. Ajima, A. Maigne, M. Yudasaka and S. Iijima, *J. Phys. Chem. B*, 2006, **110**, 19097–19099.
- 43 K. Ajima, M. Yudasaka, A. Maigne, J. Miyawaki and S. Iijima, *J. Phys. Chem. B*, 2006, **110**, 5773–5778.
- 5 44 K. Ajima, T. Murakami, Y. Mizoguchi, K. Tsuchida, T. Ichihashi, S. Iijima and M. Yudasaka, *ACS Nano*, 2008, **2**, 2057–2064.
- 45 M. R. DeWitt, A. M. Pekkanen, J. Robertson, C. G. Rylander and M. N. Rylander, *J. Biomech. Eng.*, 2014, **136**, 21003.
- 10 46 E. R. Jamieson and S. J. Lippard, *Chem. Rev.*, 1999, **99**, 2467–2498.
- 47 M. Groessel, M. Terenghi, A. Casini, L. Elviri and R. Lobinski, *J. Anal. At. Spectrom.*, 2010, **25**, 305–313.
- 48 M. D. Hall, H. R. Mellor, R. Callaghan and T. W. Hambley, *J. Med. Chem.*, 2007, **50**, 3403–3411.
- 15 49 S. Dhar, Z. Liu, J. Thomale, H. Dai and S. J. Lippard, *J. Am. Chem. Soc.*, 2008, **130**, 11467–11476.
- 50 N. Rubio, M. A. Herrero, M. Meneghetti, Á. Díaz-Ortiz, M. Schiavon, M. Prato and E. Vázquez, *J. Mater. Chem.*, 2009, **19**, 4407.
- 20 51 G. Pastorin, W. Wu, S. Wieckowski, J.-P. Briand, K. Kostarelos, M. Prato and A. Bianco, *Chem. Commun.*, 2006, 1182–1184.
- 52 C. C. Forbes, K. M. Divittorio and B. D. Smith, *J. Am. Chem. Soc.*, 2008, **128**, 9211–9218.
- 25 53 M. Adamczyk, S. R. Akireddy, P. G. Mattingly and R. E. Reddy, *Tetrahedron*, 2003, **59**, 5749–5761.
- 54 R. P. Feazell, N. Nakayama-Ratchford, H. Dai and S. J. Lippard, *J. Am. Chem. Soc.*, 2007, **129**, 8438–8439.
- 55 R. R. Traut, A. Bollen, T. Sun, J. W. B. Hershey, J. Sundberg and L. R. Pierce, *Biochemistry*, 1973, **12**, 3266–3273.
- 56 G. L. Ellman, *Arch. Biochem. Biophys.*, 1959, **82**, 70–77.
- 57 E. Venturelli, C. Fabbro, O. Chaloin, C. Ménard-Moyon, C. R. Smulski, T. Da Ros, K. Kostarelos, M. Prato and A. Bianco, *Small*, 2011, **7**, 2179–2187.
- 58 V. K. Sarin, S. B. H. Kent, J. P. Tam and R. B. Merrifield, *Anal. Biochem.*, 1981, **117**, 147–157.
- 10 59 R. Singh, L. Kats, W. A. Bla and J. M. Lambert, *Anal. Biochem.*, 1996, **236**, 114–125.
- 60 J. F. Moulder, W. F. Stickle, P. E. Sobol and K. D. Bomben, *Handbook of X-ray Photoelectron Spectroscopy*, Physical Electronics, Inc., Minnesota (United States of America), 1992.
- 15 61 A. V. Kalinkin, M. Y. Smirnov, A. I. Nizovskii and V. I. Bukhtiyarov, *J. Electron Spectrosc. Relat. Phenom.*, 2010, **177**, 15–18.
- 62 G. Glorani, R. Marin, P. Canton, M. Pinto, G. Conti, G. Fracasso and P. Riello, *J. Nanopart. Res.*, 2017, **19**, 294.
- 20 63 M. Schlapschy, U. Binder, C. Börger, I. Theobald, K. Wachinger, S. Kisling, D. Haller and A. Skerra, *Protein Eng., Des. Sel.*, 2013, **26**, 489–501.
- 64 A. Parodi, N. Quattrocchi, A. L. van de Ven, C. Chiappini¹, M. Evangelopoulos, J. O. Martinez, B. S. Brown, S. Z. Khaled, I. K. Yazdi, M. V. Enzo, L. Isenhardt, M. Ferrari and E. Tasciotti, *Nat. Nanotechnol.*, 2009, **8**, 61–68.

30

30

35

35

40

40

45

45

50

50

55

55